Modelling of brine transport in an aquifer crossing the Gorleben salt dome: Influence of initial conditions and hydrogeological settings

Peter Vogel & Klaus Schelkes
Federal Institute for Geosciences and Natural Resources (BGR)
P.O. Box 510153, 30631 Hannover, Federal Republic of Germany

The Gorleben salt dome, in the northeastern part of Lower Saxony in Germany, is under investigation as a candidate site for the final disposal of radioactive waste. The multiple-aquifer system in the sediments above the dome is in Tertiary and Quaternary sediments. The salt dome is crossed by a subglacial erosion channel, in which the lowermost Elsterian aquifer is partly in contact with the caprock or the salt itself. Saturated brines occur in these areas. These brines are overlain by a narrow transition zone in which water salinities decrease to that of brackish or fresh water. Numerical studies based on a generalized hydrogeological cross-section were conducted to determine the transient density distribution and the associated flow field in the subglacial erosion channel. The objective of these studies was to determine the effect of different hydrogeological settings and initial conditions. The transient simulations were assumed to start 10 000 years ago at the end of the last ice age. Both the initial condition and the shape of the Elsterian channel outlet to a deep Tertiary aquifer strongly affect the numerical results. Different combinations of initial conditions and hydrogeological setting may yield similar density distributions. A few of the calculated present density distributions compare well with measured field data. A unique solution to the inverse problem is not yet possible.

Introduction

In this paper, interest is focused on transient two-dimensional numerical modelling of a generalized hydrogeological cross-section along an erosion channel crossing the Gorleben salt dome. The objective was to calibrate the numerical model on the basis of the present groundwater density distribution. Paleoclimatic and hydraulic arguments yield a reasonable estimate of the rather unknown salinity distribution at the end of the last ice age to serve as initial condition. Steady-state conditions have not been reached in this groundwater system. Some of the predicted present density distributions achieve a good fit to measured density data along the entire lenth of the channel.

Hydrogeological situation

The Gorleben salt dome, in the northeastern part of Lower Saxony in Germany, is under investigation as a candidate site for the permanent disposal of radioactive waste. This salt dome is approximately 14 km long, up to 4 km wide, and its base is at a depth of more than 3000 m. Hydrogeological studies have been conducted in an area of about 300 km² around the salt dome for site characterization and long-term safety assessments. Numerous experiments have been carried out in the Gorleben area to obtain information about the hydrogeology, hydraulic parameters, and groundwater movement. A good picture of the hydrogeological situation has been obtained from these studies (Vierhuff, 1984; Fielitz et al., 1984).

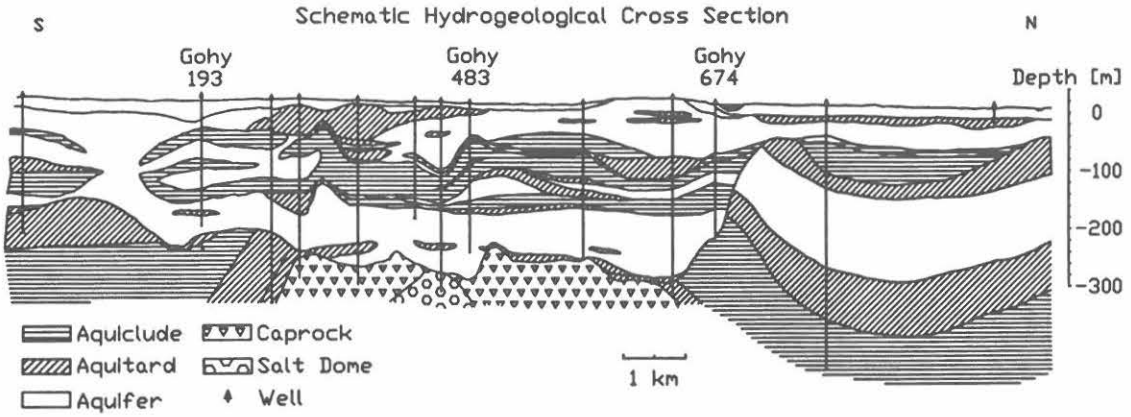

Fig. 1. Schematic hydrogeological cross-section along the Gorleben erosion channel.

Tertiary and Quaternary sediments above the Gorleben salt dome form a multiple-aquifer system up to 300 m thick. The lowermost aquifer consists of Miocene lignite-bearing sands or Elsterian sandy, gravelly deposits in subglacial erosion channels. One such channel, the so-called Gorleben erosion channel, which is more than 10 km long and 1 - 2 km wide, crosses the salt dome from south to north. This erosion channel is locally deeper than 275 m below m.s.l. and extends down to the cap rock and in some places down to the salt itself (cf. Fig. 1). The channel contains fairly thick, sandy sediments with interbedded lenses of till; these sediments are overlain by a complex of silt and clay up to 110 m thick, the Lauenburg Clay Complex. It almost completely covers the channel aquifer above the salt dome, nearly isolating it hydraulically from the shallower aquifers.

The land surface is quite flat with elevation differences of 5 - 15 m between gentle hills and the receiving streams. Below the higher elevations south of the dome, the groundwater table is about 8 m higher than the level of the discharge areas. The groundwater flows from the slightly elevated areas towards the surrounding lower regions, infiltrating almost to the salt dome at 200 - 250 m depth, where saline water is found.

Throughout the study area, the freshwater body is underlain by rather saline water. The salt content usually increases with depth. Fig. 2 (left) shows the density of water samples from the "Gorleben channel" as a func-

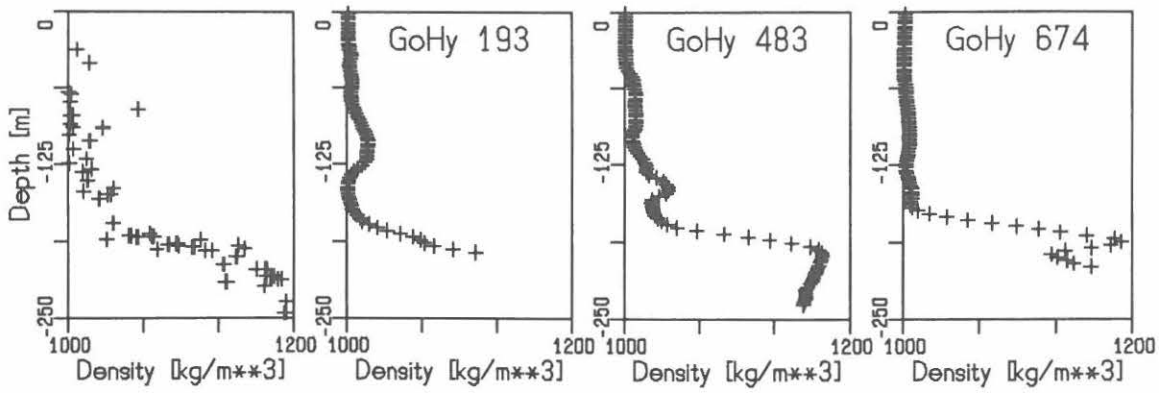

Fig. 2. Groundwater density measured on water samples (leftmost) and groundwater density logs for the wells GoHy 193, GoHy 483, and GoHy 674.

tion of depth. Induction logs were run in a number of the deeper observation wells to determine the groundwater density distribution (Ochmann & Fielitz, 1993). As an example, the groundwater density logs for three wells located on the above-mentioned cross-section are depicted in Fig. 2.

The general density distribution with depth can be characterized as follows: Groundwater mineralization increases slowly from the groundwater table down to a depth of 160 - 170 m below m.s.l. Between 170 and 200 m below m.s.l. there is a very steep increase in density from 1020 to about 1170 kg/m³. Below this transition zone highly saline water, in some places saturated brine, is found.

Simulation set-up

The schematic hydrogeological cross-section depicted in Fig. 1 was derived from the results of the hydrogeological investigation program, but it has been modified for the purpose of this numerical 2D modelling to incorporate recharge effects in the southern part of the cross-section. This modified hydrogeological cross-section served as a basis for the numerical model.

The simulated domain has a length of 16 400 m and extends from 15 m above m.s.l. down to a depth of 380 m below m.s.l. The finite element mesh employed in the simulations comprises about 4000 nodes (cf. Fig. 3).

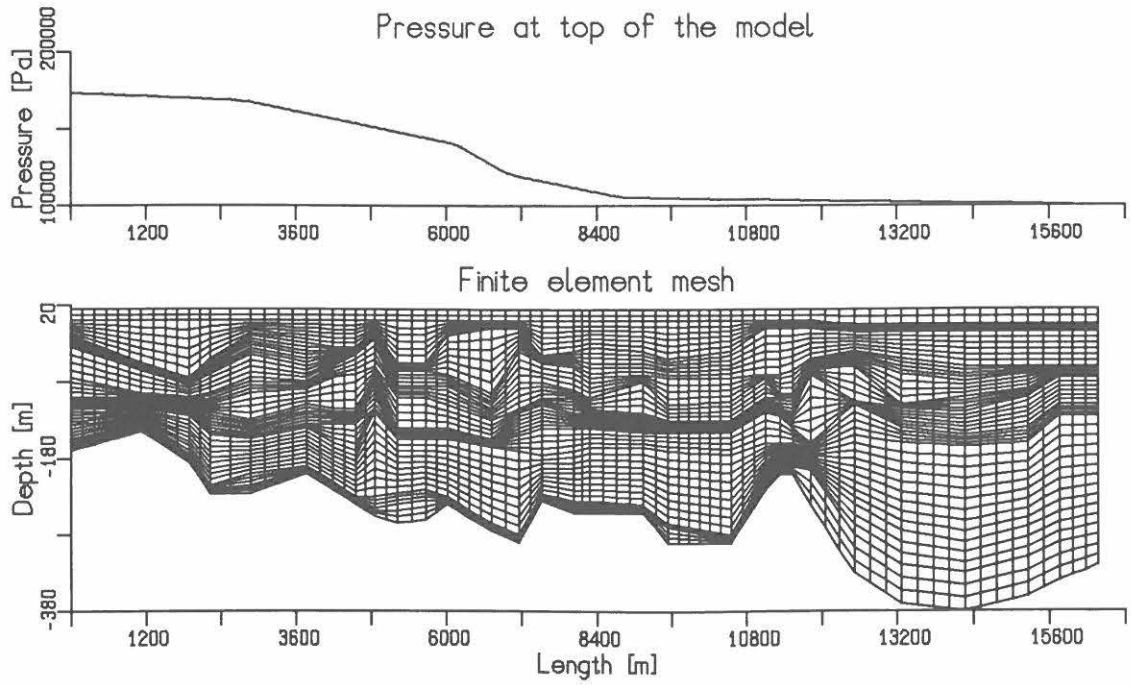

Fig. 3. Finite element mesh and pressure at top of the model.

Boundary conditions for groundwater flow and solute transport equations were chosen according to the hydrogeological situation. The pressure was fixed at the top of the cross-section to simulate the topography of the water table (top of Fig. 3). No fluid flow occurs across any other boundary. A solute concentration corresponding to that of saturated brine was assumed

along part of the bottom of the cross-section to represent the contact with the salt dome. Neither lateral boundary represents a flux boundary for solute transport. A solute concentration of zero, corresponding to fresh water, was specified along the top of the cross-section for fluid entering the system. No restriction was imposed on the solute concentration of the fluid leaving the system (i.e., free outflow).

Fluid densities were allowed to vary linearly between 1000 and 1200 kg/m^3 for solute mass fractions of 0.0 - 0.285. These values correspond to fresh water and saturated brine, respectively.

A diffusion coefficient of 10^{-9} m^2/s was used. Trial simulations showed that even small transverse dispersivities will spread any plume vertically through the entire thickness of the aquifer system within a geologically rather short time. It was also found that the system is relatively insensitive to changes in longitudinal dispersivity. Therefore, longitudinal dispersivity in each finite element was set to half of the element size and a transverse dispersivity of 0 m was employed (cf. Frind et al., 1989).

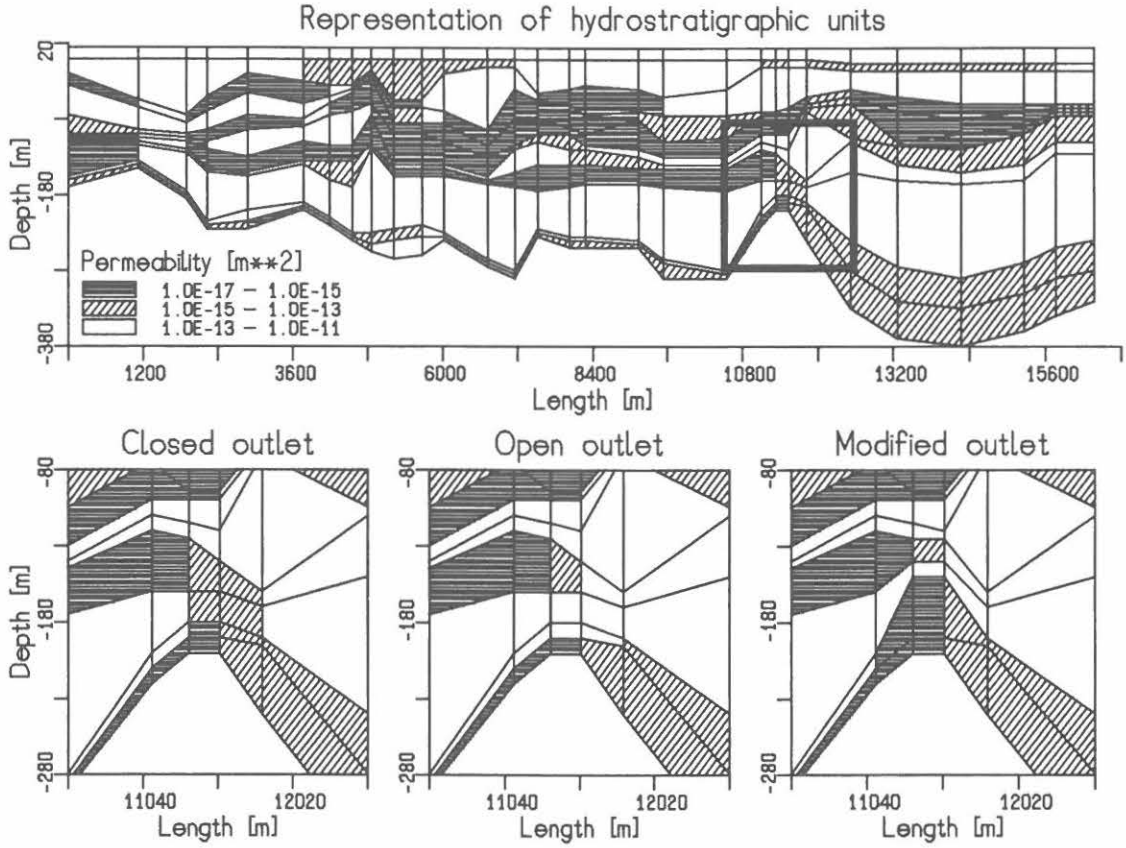

Fig. 4. Spatial orientation of the hydrostratigraphic units (top), different shapes of the channel outlet (bottom).

The numerical model can generally be characterized as a two-aquifer system consisting of aquifers, aquitards, and aquicludes with permeabilities of 10^{-12} m^2, 10^{-14} m^2, and 10^{-16} m^2, respectively, all three with a porosity of 0.2. Fig. 4 (top) depicts the permeability and spatial orientation of the hydrostratigraphic units. In the left part of the model (up to kilometer 11.5), three main layers can be distinguished. The upper one represents

the post-Elsterian aquifer system. It overlies a low-permeability zone, the Lauenburg Clay Complex. The high-permeability region below that represents the Elsterian erosion channel aquifer. At its base, contact with the diapir is assumed between kilometer six and kilometer ten. The framed area in Fig. 4 (top) depicts the northern channel outlet. Three configurations of this outlet that are equally possible within the range of currently known hydrogeological data were considered. These configurations differ in the shape and size of the channel outlet and are zoomed in Fig. 4 (bottom). The case of the closed outlet is shown in Fig. 4 (bottom left). In contrast, highly permeable elements provide a hydraulic connection to the north in the case of the open channel outlet. The hydraulic connection between the erosion channel aquifer and the area to the north is reduced in size and shifted upward for the case of the modified channel outlet. These differences in the channel outlet are the only differences between the three model geometries considered in the following discussion.

Modelling the salt water system

Numerical calculations were performed employing the SUTRA code (Voss, 1984). The objective of the investigations was to test the sensitivity of parameters and structural geometries, and to obtain a density distribution that is at least similar to the present one.

One of the main assumptions is that the present density distribution has developed since the late Pleistocene. Therefore, an important question was whether the present density distribution can be approximated by a steady-state solution. The answer had already been obtained in previous studies (Vogel et al., 1993; Schelkes & Vogel, 1993). The transient behaviour of the calculated salinity distribution indicates that steady-state conditions have not yet been reached in the observed groundwater system. The initial salinity distribution and the modelled time period strongly affect the simulation results.

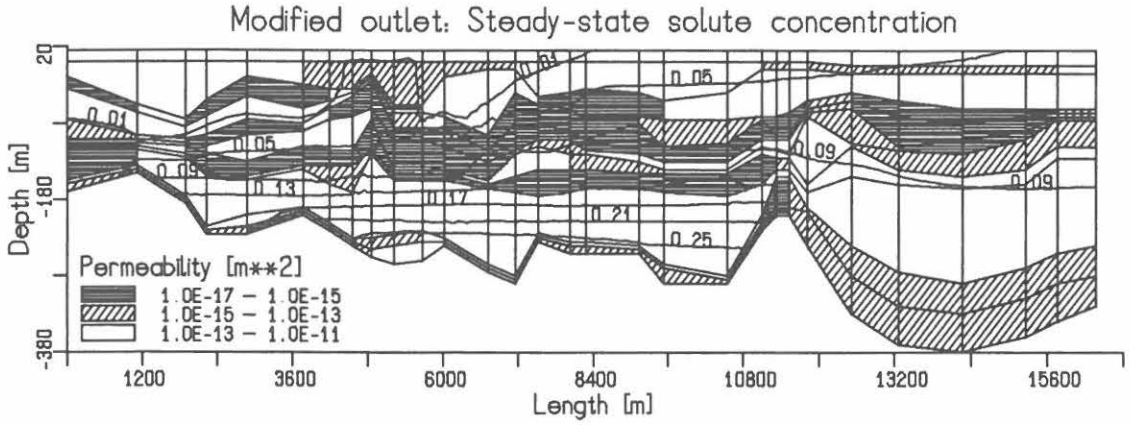

Fig. 5. Calculated steady-state concentration.

To verify this result for the cross-section under investigation, the steady-state salinity distribution was approximated by long-term transient simulations. The results of the numerical modelling are depicted in Fig. 5. Apart from a freshwater lens in the recharge area, brackish water is found up to the top of the model. Instead of the observed steep density increase within a small transition zone, the results exhibit an only moderate

salinity increase spread over the entire thickness of the lower channel aquifer. This confirms the earlier results that the observed density distribution cannot be obtained by a steady-state solution.

Therefore, a transient solution method was selected. This requires the setting of the initial conditions and the time period to be modelled. With respect to the paleoclimatic history, it was assumed that the simulations start at the end of the last ice age, approximately 10 000 years ago, and end at the present. This assumption requires a reasonable estimate of the rather unknown former density distribution to serve as an initial condition. On the basis of the hypothesis that the groundwater was mainly at rest during the last ice-age, the estimated initial density distributions were assumed to be hydraulically stable, i.e., density increases with depth. Due to dissolution, saturated brines were assumed to prevail at least in that area where the groundwater is in contact with the diapir. The present density distribution is characterized by deep brines in the lowermost channel aquifer, overlain by a transition zone with water salinities decreasing to that of brackish or fresh water. Therefore, it seemed reasonable to start the simulation runs with initial solute concentrations that exhibit a similar characteristic feature.

All initial conditions investigated assume saturated brine at the base with freshwater conditions prevailing throughout the remaining modelled area. A small horizontal transition zone separates the two regions. The depth of this narrow transition zone was varied in a series of simulation runs. Saturated brines always prevail at the base of the lower channel aquifer. Depending on the depth of the transition zone and the depth of the channel outlet in some cases, the brine/freshwater interface was extended to the north, where field data on groundwater densities are not yet available. Fig. 6 presents a schematic sketch of the initial density distributions. The different positions of the transition zone are indicated by thick lines.

For each of the three model geometries, the conditions from 10 000 years ago to the present were simulated. Special care was taken to match the depth and size of the present transition zone in the lower channel aquifer. The measured densities of water samples and the three measured density logs shown in Fig. 2 were selected as reference.

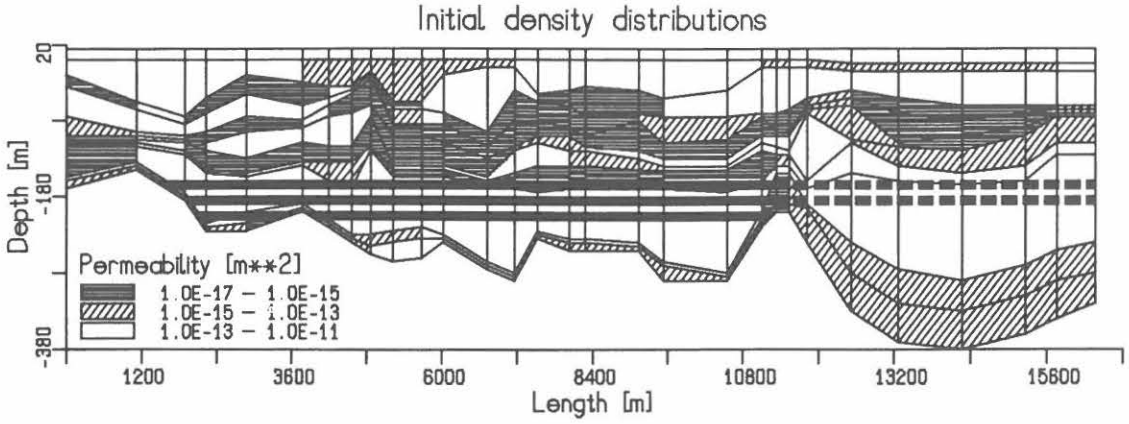

Fig. 6. Schematic sketch of initial conditions indicating positions of the brine/freshwater transition zone.

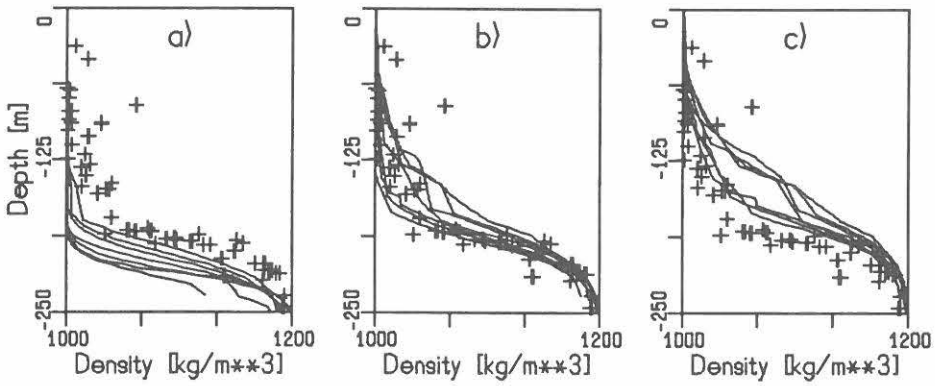

Fig. 7. Comparison of measured water samples densities with calculated density distributions employing different initial conditions. The initial brine/freshwater transition zone is a) in lower, b) in medium, c) in upper position.

Vertical density distributions at equally spaced locations between kilometers 4.5 and 10.5 in the model were compared with the densities of the water samples. These calculated densities are shown as solid lines together with the measured water densities in Fig. 7. All simulations that employ the initial brine/freshwater interface in the lowermost position predict a depth of the transition zone below the observed one (Fig. 7a). Similarly, all simulations that employ the initial brine/freshwater interface in the uppermost position predict a depth of the transition zone above the observed one (Fig. 7c). Thus, the range of possible initial conditions could be reduced. Only those cases were investigated further that start from a

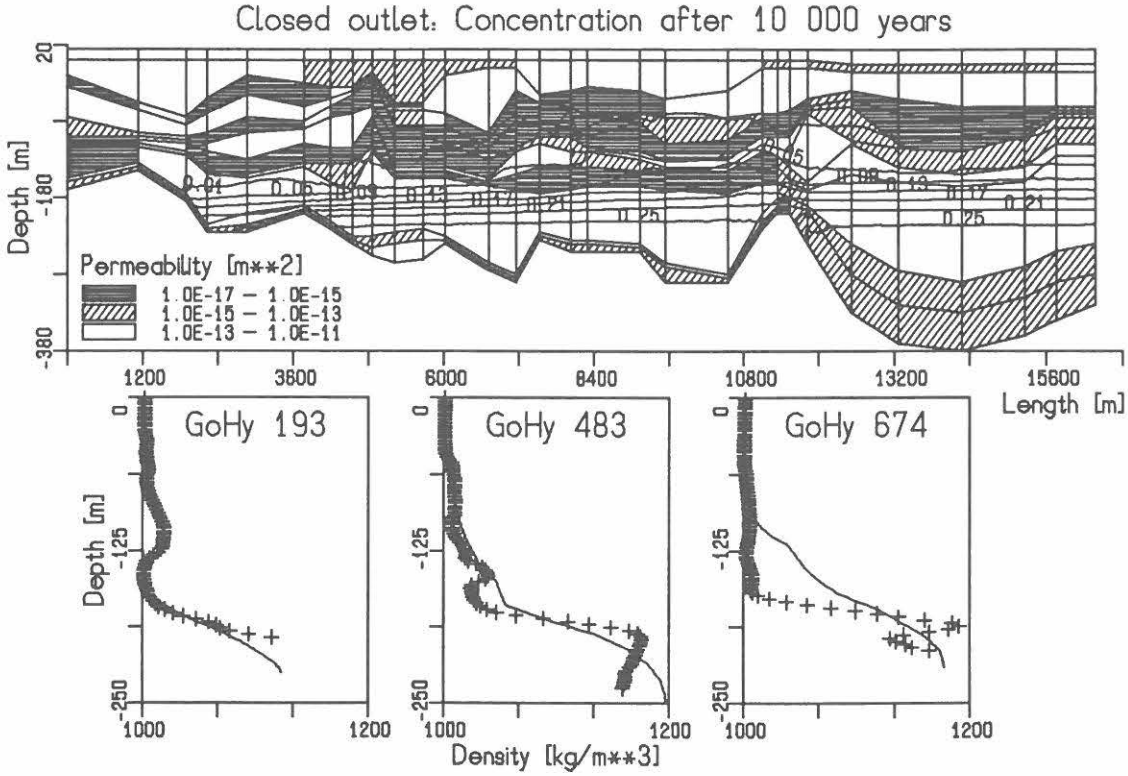

Fig. 8. Closed channel outlet: Calculated solute concentration (top), comparison of measured and calculated density logs (bottom).

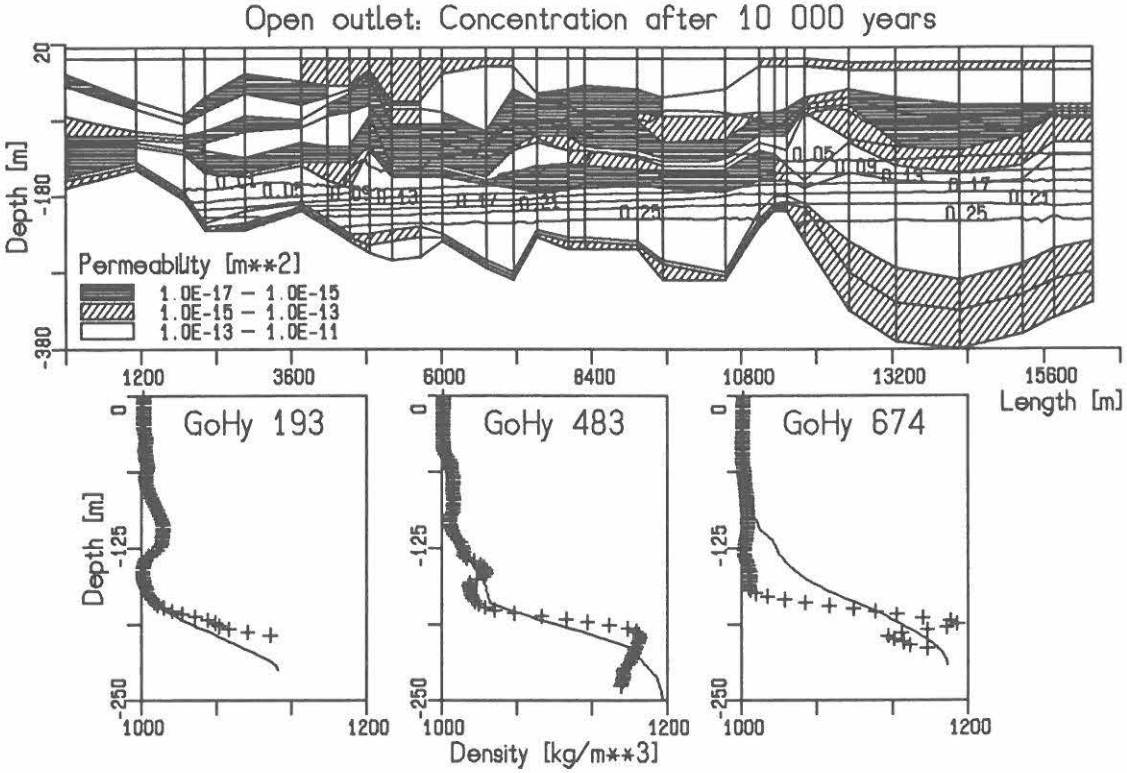

Fig. 9. Open channel outlet: Calculated solute concentration (top), comparison of measured and calculated density logs (bottom).

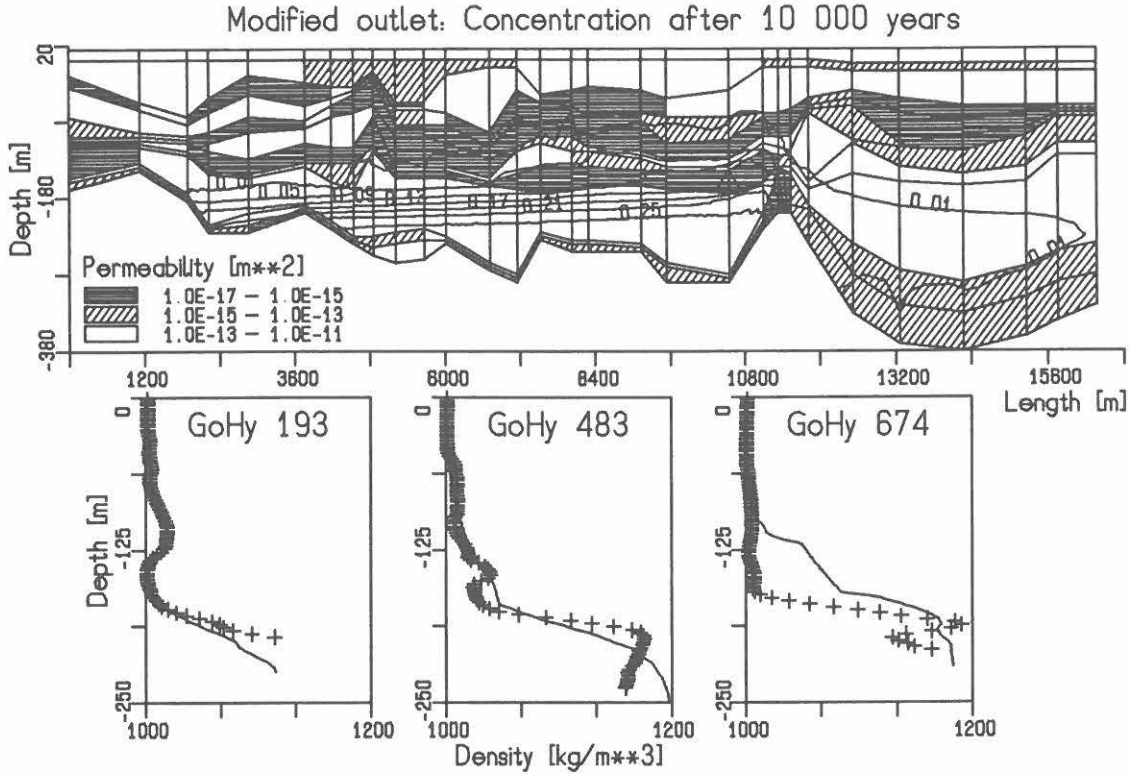

Fig. 10. Modified channel outlet: Calculated solute concentration (top), comparison of measured and calculated density logs (bottom).

somewhat medium depth of the initial brine/freshwater interface and yield results similar to those in Fig. 7b.

However, plots like in Fig. 7 do not allow decisions to be made about which is the best fit. Hence, a more detailed criterion had to be provided for the further investigations. The three wells GoHy 193, GoHy 483, and GoHy 674 are located exactly on the cross-section under investigation. They are spaced over the entire length of the channel (Fig. 1) and there are measured density logs available for these wells (Fig. 2). Therefore, the next step was to achieve a fit of the calculated density distributions to the measured density logs at these three well locations.

For this purpose, the previous estimates of suitable initial conditions were gradually improved. A set of initial conditions was thus obtained that all fit the simulation results to the measured density logs. These initial conditions have in common the initial depth of the brine/freshwater interface, but they differ in its lateral extent. Figs. 8 to 10 present the best-fit results for each of the model geometries. The predicted solute distributions are shown at the top. A comparison of the three measured density logs with the simulation results (solid lines) is presented at the bottom. Generally, measured and calculated densities are in fairly good agreement for wells GoHy 193 and GoHy 483 and are in still acceptable agreement for well GoHy 674. The results for the three model geometries are very similar to each other. Hence, a set of solutions is obtained that compare more or less favourably to the measured density logs but the best of them cannot yet be established.

The lateral extent of the initial brine/freshwater interface is easily inferred from the plots of the calculated solute distributions in Figs. 8 to 10. In the case of the modified outlet, this interface was restricted to the channel itself. In the cases of the closed and the open channel outlets, the initial interface was extended to the right (i.e., to the north). Comparison of calculated and measured groundwater densities north of the channel could help reduce ambiguity in the simulation results. Although there is considerable groundwater density data available for the erosion channel and surrounding area, the current database does not yet provide information on groundwater densities further to the north. This lack of information is one of the reasons why a unique solution to the inverse problem cannot be given at present.

REFERENCES

FIELITZ, K., GIESEL, W., SCHELKES, K. & SCHMIDT, G., 1984: Calculations of Groundwater Movement and Salt Transport in the Groundwater of the Sedimentary Cover of the Gorleben Salt Dome. - Proc. Int. Symp. on Groundwater Utilisation and Contaminant Hydrogeology, Montreal, Canada, Vol. II, pp. 383-392. AECL.

FRIND, E.O., DUYNISVELD, W.H.M., STREBEL, O. & BÖTTCHER, J., 1989: Simulation of Nitrate and Sulfate Transport and Transformation in the Fuhrberger Field Aquifer, Hannover, Germany. In H.E. Kobus & W. Kinzelbach: Proc. Int. Symp. on Contaminant Transport in Groundwater, Stuttgart, Germany, pp. 97 - 104. - Balkema. Rotterdam, Brookfield.

OCHMANN, N. & FIELITZ, K., 1993: Estimation of Horizontal and Vertical Groundwater Flow from Well-Logging and Pressure Data in Groundwater of Variable Density above a Salt Dome. In E. Custodio & A. Galofré: Study and

Modelling of Salt Water Intrusion into Aquifers, Proc. 12th Salt Water Intrusion Meeting, Barcelona, pp. 23-34. - CIMNE. Barcelona.

SCHELKES, K. & VOGEL, P., 1993: Paleohydrogeological Information as an Important Tool for Groundwater Modeling of the Gorleben Site. In: Paleohydrogeological Methods and their Applications, pp. 237-250. - OECD. Paris.

VIERHUFF, H., 1984: Hydrogeological Investigations in the Area of the Gorleben Salt Dome. - Proc. Int. Symp. on Groundwater Utilisation and Contaminant Hydrogeology, Montreal, Canada, Vol. II, pp. 573-579. AECL.

VOGEL, P., SCHELKES, K. & GIESEL, W., 1993: Modeling of Variable-Density Flow in an Aquifer Crossing a Salt Dome - First Results. In E. Custodio & A. Galofré: Study and Modelling of Salt Water Intrusion into Aquifers, Proc. 12th Salt Water Intrusion Meeting, Barcelona, pp. 359-369. - CIMNE. Barcelona.

VOSS, C.I., 1984: Sutra: A Finite-Element Simulation Model for Saturated Unsaturated, Fluid-Density-Dependent Ground-Water Flow with Energy Transport or Chemically-Reactive Single Species Solute Transport. - USGS Water Resour. Invest. Rep. 84-4369.